

# Crossing and anticrossing of spin-split Landau levels in an $\text{Al}_x\text{Ga}_{1-x}\text{As}/\text{GaAs}$ parabolic quantum well ferromagnet

G. Yu,<sup>1,2</sup> D. J. Lockwood,<sup>1</sup> A. J. SpringThorpe,<sup>1</sup> and D. G. Austing<sup>1</sup>

<sup>1</sup>*Institute for Microstructural Sciences, National Research Council of Canada, Ottawa, Ontario, Canada K1A 0R6*

<sup>2</sup>*National Laboratory for Infrared Physics, Shanghai Institute of Technical Physics, Chinese Academy of Science, Shanghai 200083, People's Republic of China*

(Received 29 March 2007; revised manuscript received 27 June 2007; published 17 August 2007)

An electric field modulation technique is used to measure directly the second derivative with respect to gate voltage of Shubnikov–de Haas oscillations for an  $\text{AlGaAs}/\text{GaAs}$  parabolic quantum well with two spatially coincident populated subbands. This technique resolves the spin-split regions in the topological phase diagram and allows observation of the two-subband Landau fan diagram in fine detail. We observe, and model with an effective  $g$  factor, the curved Landau levels of the first and second subbands in a tilted magnetic field. We obtain evidence for intersubband mixing, but the details are not in accord with present theory. For certain applied electric and magnetic fields, quantum Hall ferromagnetic ground states are also observed.

DOI: [10.1103/PhysRevB.76.085331](https://doi.org/10.1103/PhysRevB.76.085331)

PACS number(s): 73.21.Fg, 73.63.Hs, 73.43.-f, 71.70.Di

## I. INTRODUCTION

An  $\text{AlGaAs}/\text{GaAs}$  parabolic quantum well (PQW) is an interesting structure for spintronics because of the ability to change the PQW  $g$ -factor magnitude and sign with an applied electric field.<sup>1–3</sup> Additionally, phenomena, such as ferromagnetism and level mixing, related to the crossing and anticrossing of either spatially coincident or spatially separate spin-split Landau levels (LLs) or LL related one- or zero-dimensional states have also attracted much attention not just for PQWs<sup>4–8</sup> but also for heterojunction, square quantum well, quantum wire, and quantum dot systems.<sup>9–15</sup> The energy level problem for a two-dimensional electron gas in a tilted magnetic field was solved analytically, in the absence of Coulomb interactions, for wide PQWs by Mann<sup>16</sup> and Merlin.<sup>17</sup> Merlin showed that LLs of the first subband develop negative curvature with increasing magnetic field, while LLs of the second subband show positive curvature. Therefore, it is possible to observe both crossings and anticrossings between the two sets of LLs.

Intersubband transitions were originally detected in conventional square quantum wells (QWs) at infrared frequencies via cyclotron resonance in a tilted magnetic field<sup>18–20</sup> and also by Raman scattering.<sup>21</sup> However, spin-splitting effects were neither considered in the theory nor observed in these optical experiments. More recently, spin-flip transitions at points where spin-split LLs of the first and second subbands cross in square QWs have been studied by Hall measurements.<sup>11,14</sup> Contrary to the optical investigations, these experimental efforts focused on low temperature ( $<1$  K) studies of high-mobility heterostructures in a magnetic field normal to the sample.

We have previously investigated the electron transport and quantum mobilities of an  $\text{Al}_x\text{Ga}_{1-x}\text{As}/\text{GaAs}$  PQW with two populated subbands by analyzing the fast Fourier transform spectra.<sup>22</sup> We found that the transport mobility is relatively low at around  $3 \times 10^4$   $\text{cm}^2/\text{V s}$  for low electron density ( $\sim 2 \times 10^{15}$   $\text{m}^{-2}$ ) when the first subband only is occupied, and it increases with increasing electron density although nonlinearly when the second subband becomes oc-

cupied due to intersubband scattering. In this paper, we use an electric field modulation technique to better resolve the phase diagram of the spin splitting at odd Landau filling factors in such PQWs, and have thereby mapped out the topological phase diagram in the electron density–magnetic field plane for crossing and anticrossing LLs. Crossing LLs can occur for any magnetic field tilt angle  $\theta$  (between the field and the normal to the sample), including  $\theta=0$ , and anticrossing LLs can be induced with a finite tilt angle (we employ large angles). We obtain clear LL fan diagrams as a function of magnetic field for both the first and second subbands. We observe in a PQW, particularly well at  $\theta=0$ , the quantum Hall ferromagnetic ground state originally seen in square QWs<sup>9,11,14</sup> and more recently in a PQW.<sup>7</sup> In a tilted field, we observe the predicted intersubband coupling, which can cause anticrossings, in the region where two subbands mix.

The sample and experimental details are described in Sec. II. The results and discussion are presented in Sec. III along with an illustration of the differences between our measurement technique and more conventional transport measurements. Conclusions are given in Sec. VI.

## II. SAMPLE AND EXPERIMENTAL DETAILS

The sample measured is an  $\text{Al}_x\text{Ga}_{1-x}\text{As}/\text{GaAs}$  PQW grown by molecular beam epitaxy.<sup>22</sup> On top of the semi-insulating GaAs substrate, the following layers were grown: a 100 nm undoped GaAs buffer layer, a ten period AlAs (five monolayers)/GaAs (ten monolayers) undoped superlattice, a 250 nm undoped GaAs layer, a 150 nm undoped  $\text{Al}_{0.29}\text{Ga}_{0.71}\text{As}$  layer, a thin region Si-delta-doped to  $5.0 \times 10^{15}$   $\text{m}^{-2}$ , a 15 nm undoped  $\text{Al}_{0.29}\text{Ga}_{0.71}\text{As}$  layer, the 100-nm-wide  $\text{Al}_x\text{Ga}_{1-x}\text{As}$  PQW with  $x$  varied parabolically and *continuously* (not digitally) from 0.29 to 0 (in the middle of this layer) and back to 0.29, a 15 nm undoped  $\text{Al}_{0.29}\text{Ga}_{0.71}\text{As}$  layer, a thin region Si-delta-doped to  $5.0 \times 10^{15}$   $\text{m}^{-2}$ , a 35 nm undoped  $\text{Al}_{0.29}\text{Ga}_{0.71}\text{As}$  layer, and finally, a 10 nm undoped cap GaAs layer.

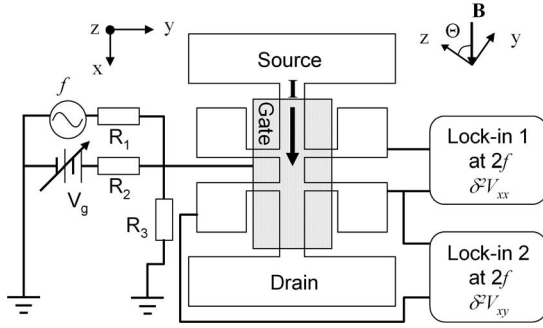


FIG. 1. Diagram of the experimental setup for the electric-field-modulated Hall effect. The sense of the magnetic field tilt (accurate to  $\sim 1^\circ$ ) is indicated ( $R_1=R_2=1\text{ k}\Omega$ ,  $R_3=100\ \Omega$ ).

After growth, the PQW structure was processed into a standard Hall bar with a front gate. The distance between the voltage probes was  $400\ \mu\text{m}$  and the width of the bar was  $200\ \mu\text{m}$ . Transport measurements were made at  $1.3\text{ K}$  in a magnetic field up to  $8\text{ T}$  (always swept from low to high field). Figure 1 is a schematic view of the sample and our experimental geometry. A dc of  $I=200\text{ nA}$  was passed from the source to the drain, and dc and ac voltages were applied to the front gate. In this case, the longitudinal (transverse Hall) voltage  $V_{xx}$  ( $V_{xy}$ ) can be written as

$$\begin{aligned}
 V_{xx,xy}(V_g) &= IR_{xx,xy}(V_g) \\
 &= V_{xx,xy}(V_{g0}) + \frac{dV_{xx,xy}}{dV_g} a \sin(2\pi ft) \\
 &\quad + \frac{1}{2} \frac{d^2 V_{xx,xy}}{dV_g^2} [a \sin(2\pi ft)]^2 + \dots \\
 &= V_{xx,xy}(V_{g0}) + \frac{1}{4} \frac{d^2 V_{xx,xy}}{dV_g^2} a^2 + \frac{dV_{xx,xy}}{dV_g} a \sin(2\pi ft) \\
 &\quad - \frac{1}{4} \frac{d^2 V_{xx,xy}}{dV_g^2} a^2 \cos(4\pi ft) + \dots, \quad (1)
 \end{aligned}$$

where  $f=20\text{ Hz}$  is the frequency of the ac gate voltage and  $a=1\text{ mV}$  its amplitude. We use two lock-in amplifiers synchronized at frequency  $2f$  (see Fig. 1) to measure the change in the voltage  $\delta^2 V_{xx,xy} = (1/4)(d^2 V_{xx,xy}/dV_g^2)a^2$ .

### III. RESULTS AND DISCUSSION

For our experimental situation, we found it convenient and useful to measure the variations  $\delta^2 V_{xx}$  and  $\delta^2 V_{xy}$  with respect to the gate voltage. Because this measurement technique may be unfamiliar, we first illustrate the differences between it and more conventional transport measurements. Typical results for the simple case of single subband occupation for resistances  $R_{xx}$  and  $R_{xy}$  (obtained in the same manner as in Ref. 22), and the variations  $\delta^2 V_{xx}$  and  $\delta^2 V_{xy}$  with respect to the gate voltage modulation for zero tilt angle are shown in Fig. 2 as a function of magnetic field. To comprehend the variation of the directly measured second derivative

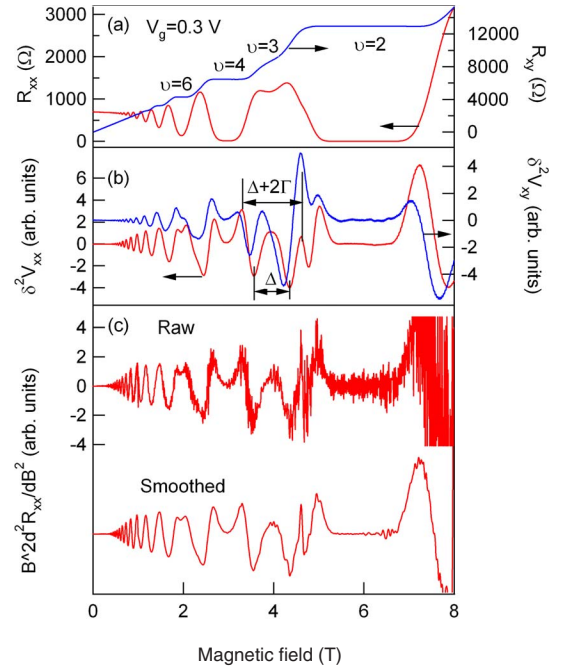


FIG. 2. (Color online) (a) Typical traces, here for first subband only occupation, of the resistances  $R_{xx}$  and  $R_{xy}$  versus the magnetic field for zero tilt angle. The Landau filling factors  $\nu$  are indicated. (b) The variation of voltage  $\delta^2 V_{xx}$  and  $\delta^2 V_{xy}$  as a function of the magnetic field measured under the same conditions as  $R_{xx}$  and  $R_{xy}$ . The  $\Delta$  and  $\Delta+2\Gamma$  separations are marked for  $\nu=3$ . (c) Quantity  $B^2 d^2 R_{xx}/dB^2$  versus magnetic field, derived from the  $R_{xx}$  data shown in (a), raw and smoothed.

result,  $\delta^2 V_{xx}$ , the similar but “noisier” quantity  $B^2 d^2 R_{xx}/dB^2$  conventionally derived numerically<sup>23</sup> from the raw  $R_{xx}$  is also shown in Fig. 2 as a function of magnetic field. If  $R_{xx}$  is smoothed, this quantity then resembles  $\delta^2 V_{xx}$ . To illustrate what information can be obtained from the second derivative results, we model  $R_{xx}$  in the vicinity of filling factor  $\nu=3$  [see Fig. 2(a)] with two overlapping Lorentzian peaks, corresponding to the spin-up and spin-down LLs, each of width  $\Gamma$  and separated by  $\Delta$ . After taking the second derivative of such a pair of peaks, we can, when  $\Delta > \Gamma$ , obtain four peaks, in which the inner two separated by  $\Delta$  are pointing downward and the outer two separated by  $\Delta+2\Gamma$  are pointing upward. Therefore, when we experimentally observe pairs of upward peaks with this technique [see Fig. 2(b)], we have effectively “expanded” the spin-splitting region of odd Landau index  $\nu$ , and correspondingly, “shrunk” the region of even  $\nu$ . Note from the example traces in Fig. 2(b),  $\Delta \approx 0.79\text{ T}$  for the  $\nu=3$  spin splitting, from which we obtain an effective  $g$ -factor for the first subband,  $|g^*| \approx 9$ , taking an effective mass  $m^* = 0.067m_e$ , which we use in our model discussed below. We found our second derivative technique particularly useful for the more complex case of two subband occupations.

Next, numerous scans were taken by fixing the gate voltage  $V_g$  and sweeping the magnetic field, producing a Landau fan diagram of  $\delta^2 V_{xx}$  as shown in Fig. 3(a), where the tilt

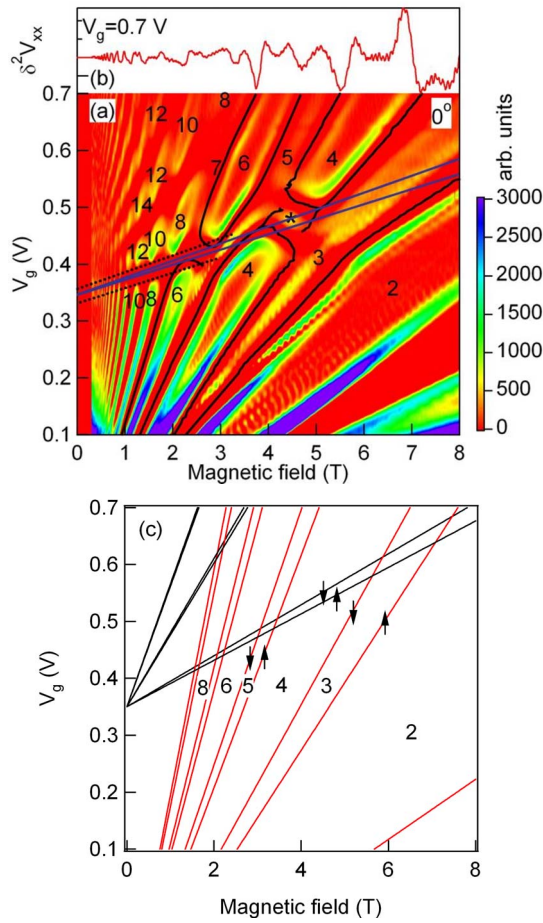


FIG. 3. (Color online) (a) Fan chart of  $\delta^2 V_{xx}(B, V_g)$  data for zero tilt angle with step of 0.01 V in  $V_g$ . Red areas indicate zero and negative values of  $\delta^2 V_{xx}$ , and the color changes from yellow to green to blue as  $\delta^2 V_{xx}$  becomes more positive. The solid lines mark the positions of relevant negative peaks in  $\delta^2 V_{xx}$ , and the filling factor  $\nu$  is indicated by the numbers. The dotted black lines show the expanded spin splitting  $\Delta + 2\Gamma$  for the second subband lowest level, while the blue solid lines between the dotted black lines denote the estimated  $\Delta$ . The center of the  $\nu=4$  ringlike structure is marked with an asterisk. (b)  $\delta^2 V_{xx}$  trace for  $V_g=0.7$  V clearly showing the relevant negative peaks associated with the solid lines marked in (a). (c) The calculated fan chart for zero tilt. The up and down arrows denote the electron spin states of the spin split LLs.

angle of the magnetic field is zero. The trace at  $V_g=0.7$  V is shown in Fig. 3(b) as an example. It is clear that there are gaps in the mixed regions between the first- and second-subband LLs, and this is most clear for the  $\nu=4$  quantum Hall state in the vicinity of  $V_g=0.5$  V (position marked by asterisk). The evolution of the  $\nu=4$  state in both  $R_{xx}$  and  $R_{xy}$  as the gate voltage is swept from  $V_g=0.44$  to 0.56 V is shown in Figs. 4(a) and 4(b). This phenomenon was originally explained for nonparabolic QWs.<sup>11,14</sup> In the vicinity where two spin-split LLs with different subband indices cross each other, there is a high probability to form, for even- $\nu$ , aligned electron spins in order to gain exchange energy. Such an ordered quantum Hall ferromagnetic ground

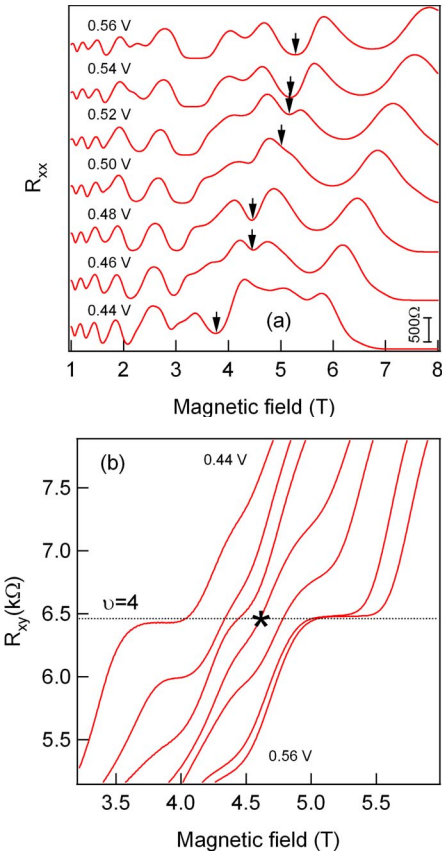


FIG. 4. (Color online) (a)  $R_{xx}$  and (b)  $R_{xy}$  near  $V_g=0.5$  V (step in  $V_g=0.02$  V) in the vicinity of the “ring,” whose center is marked with an asterisk in Fig. 3(a). The arrows in  $R_{xx}$  mark the  $\nu=4$  quantum Hall state, which is clearly modulated in strength around  $V_g=0.48$  V. The  $R_{xx}$  curves have been offset for clarity and each curve is labeled with the gate voltage. The modulation of the  $\nu=4$  state is also apparent in corresponding  $R_{xy}$  curves. The asterisk on the  $V_g=0.48$  V curve at  $\nu=4$  emphasizes the link with the fan chart data in Fig. 3(a); the gaps themselves are to the left and right of the asterisk.

state has been observed in transport measurements, for example, on a 60-nm-wide square GaAs quantum well at 0.33 K with a  $V_g=0$  V mobility of  $\sim 2.6 \times 10^6$  cm<sup>2</sup>/V s,<sup>9</sup> subsequently on a 40-nm-wide square GaAs quantum well at 0.05 K with a mobility of  $\sim 4.0 \times 10^6$  cm<sup>2</sup>/V s,<sup>11</sup> on a 24-nm-wide square GaAs quantum well at 0.34 K with a mobility of  $\sim 4.1 \times 10^5$  cm<sup>2</sup>/V s,<sup>14</sup> and most recently, on a 100-nm-wide PQW at 0.1 K with a mobility of  $\sim 1.6 \times 10^5$  cm<sup>2</sup>/V s.<sup>7</sup> The  $\nu=4$  “ringlike” structure we see between 4 and 5 T in Fig. 3(a) is also a direct evidence of the existence of multiple phases with the same quantized Hall conductance,<sup>7,11,14</sup> and thus, the ferromagnetic phase has been confirmed here with our technique for a 100-nm-wide PQW sample even with a low mobility ( $\sim 1 \times 10^4$  cm<sup>2</sup>/V s) and at a relatively high temperature (1.3 K) for the quantum Hall effect measurements. Note that while the  $\nu=4$  ringlike structure is clearest, we do see other smaller “rings” in Fig. 3(a), e.g., at  $\nu=6$ . Interestingly, the details of the  $\nu=4$

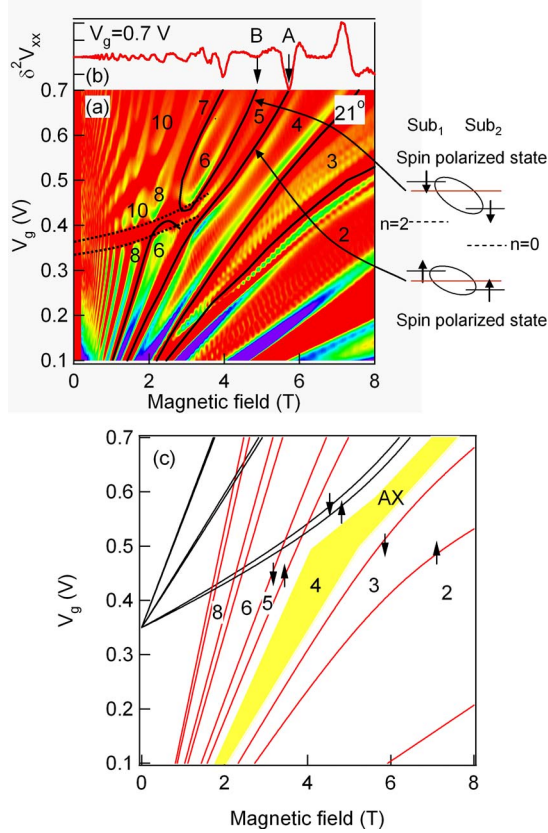


FIG. 5. (Color online) (a) Fan chart of  $\delta^2 V_{xx}$  in a tilted magnetic field of  $21^\circ$  constructed similar to the one in Fig. 3(a). The cartoon pictorially shows the “mixing” between the spin-up (spin-down) states of the third ( $n=2$ ) LL of the first subband and the first ( $n=0$ ) LL of the second subband, giving rise to the line marked A (B). (b)  $\delta^2 V_{xx}$  trace for  $V_g=0.7$  V, again clearly showing the relevant negative peaks associated with the solid lines marked in (a). (c) The calculated fan chart for this angle revealing the anticrossing (AX) for  $\nu=4$ .

ringlike structure are seen to be different from those of higher index rings in Refs. 11 and 14 on square quantum wells. Below we describe the details of the calculation for the fan chart shown in Fig. 3(c) for zero tilt, but we note first, as expected, that there are no anticrossings, and second, since the model is single particle in nature, the observed ring structure is not reproduced as is well discussed in Ref. 14.

Further interesting physical features emerge in the  $\delta^2 V_{xx}$  data for tilted magnetic fields. Data obtained for a tilt angle of  $21^\circ$  are shown in Figs. 5(a) and 5(b), and the calculated LLs using Merlin’s single-particle PQW model<sup>17</sup> are shown in Fig. 5(c). For the theoretical calculations, the additional spin splittings were calculated from  $\Delta = g_0 \mu_B B + (g^* - g_0) \mu_B B_\perp$ , taken from Ref. 24, where the GaAs bulk  $g$  factor  $g_0 = -0.44$ ,  $\mu_B$  is the Bohr magneton, and  $B$  and  $B_\perp = B \cos(\theta)$  are the total magnetic field and its perpendicular component, respectively. An “exchange enhanced”  $g$  factor ( $g^*$ ) is a common means to phenomenologically add complex exchange effects to the single-particle picture of LLs.<sup>7,8,14,24</sup> We take the effective  $g$  factor  $|g^*| = 9$  for the first subband (see above), and we estimate from the spin splitting of the second subband [see the dotted black lines and solid lines (blue

online) between the dotted black lines in Fig. 3(a)]  $|g^*|$  for the second subband to be  $\sim 1.8$ . Note that the sign of the first and second subband  $g^*$  values is assumed to be the same as that of  $g_0$ . We also assumed that the Fermi energy is linearly related to the gate voltage. From  $m^*$ , and the electron density of  $3.1 \times 10^{15} \text{ m}^{-2}$  for  $V_g = 0.35$  V at which the second subband starts to be occupied, we obtain  $E_{12} = 11$  meV for the spacing between the first and second subbands at 0 T, which is in good agreement with our previous results.<sup>22</sup> A clear anticrossing of LLs is observed experimentally at a tilt angle of  $21^\circ$  in Fig. 5(a) for a magnetic field near 5 T at  $\nu=4$ , and this is confirmed from the simple Merlin model [marked AX at  $\sim 6$  T in Fig. 5(c)]. Note again that there is only qualitative agreement with the single-particle model; i.e., the AX is reproduced, but discrepancies in the field dependence of the fan, as in the zero tilt case, are evident.

On further analyzing the data obtained for a tilt angle of  $21^\circ$ , we notice the following interesting observations. The  $\nu=6$  region near  $B=3$  T and  $V_g=0.4$  V has arisen from a crossing of spin-split LLs in a similar way as the  $\nu=4$  ring-like structure shown in Fig. 3(a) for zero tilt angle, although it is not as clearly defined. On the high field side of this structure, rather than seeing a clear continuation of the four first and second subband LL states, only two single minima in  $\delta^2 V_{xx}$  are observed; i.e., the expected spin-split pairs appear to be unresolved and we see just two lines marked as A and B in Fig. 5(a). We believe that this behavior can be explained in terms of “mixing” of odd- $\nu$  same-spin states originating from the two Landau fans as postulated in Ref. 11. By mixing we mean levels in close proximity merge (see cartoon). The single minimum observed at both the low (line B) and high (line A) field sides of the  $\nu=5$  state beyond 3 T, which arises from these mixed same-spin states, cannot be accounted for by the Merlin model shown in Fig. 5(c) because of its single-particle nature.

Similar anticrossings are predicted for  $\nu=6$  at a field near 6 T for a tilt angle of  $45^\circ$ , and likewise for  $\nu=8$  above  $\sim 6$  T at  $61^\circ$  tilt [see Figs. 6(b) and 7(b)]. Experimentally, while the anticrossings are less clear at these larger tilt angles, we do see the characteristic negative curvature of several of the first subband LLs as well as the positive curvature of the second subband LLs [see Figs. 6(a) and 7(a)]. To emphasize that a high first subband  $g^*$  value is needed to reproduce best our data, we give in Fig. 7(b) the calculated fan chart for a first subband effective  $g$  factor  $|g^*| = 9$  and take  $|g_0| = 0.44$ . Note that the calculated fan chart would have reproduced poorly the experimental data had we used either  $|g^*| = 0$  or  $|g^*| = 2$ . These situations correspond, respectively, to using just the bulk  $g$  value for GaAs and a  $g^*$  value widely used for quantum wells. Thus for overall agreement between the theory and experiment, i.e., considering the whole fan chart and not just in the vicinity of specific features such as the ring structure, we clearly see the need for a high  $g^*$  value. Our calculations show this to be most apparent at a high tilt angle where large spin splittings were experimentally seen, whereas at lower tilt angle this was less evident.

From our work on PQWs, it is clear that the single-particle picture including exchange interactions phenomenologically, through the use of an enhanced  $g$  factor,  $g^*$ , is not sufficient to explain all the observed details such as the ring

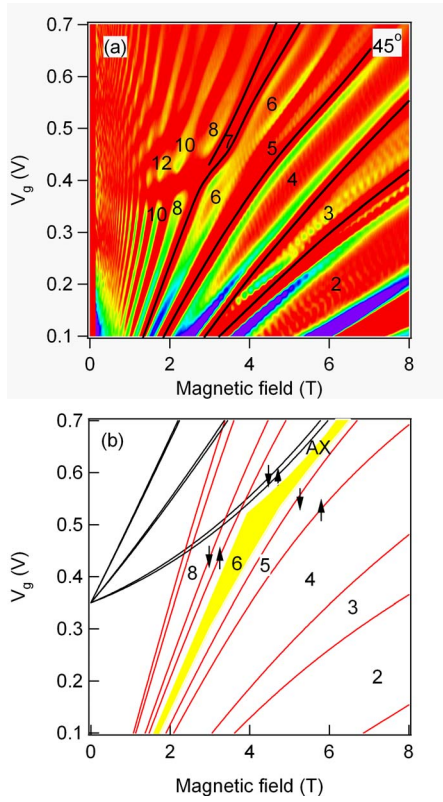


FIG. 6. (Color online) (a) Fan chart of  $\delta^2 V_{xx}$  in a tilted magnetic field of  $45^\circ$  constructed similar to the one in Fig. 3(a). (b) The calculated fan chart for this angle revealing the anticrossing (AX) for  $\nu=6$ .

structures and the precise details of the LL field dependence. In this regard, it would be interesting to ascertain why we had to take such a high  $g^*$  value for the first subband, while for the second subband a much smaller value was necessary to obtain general agreement between experiment and theory in the LL mixing regions shown in Figs. 5–7.<sup>7</sup> In addition, our results appear to confirm the assumptions and conclusions of previous work<sup>24</sup> regarding the spin-splitting variation with tilted magnetic fields. For example, only the part  $g_0\mu_B B$  of the spin splitting  $\Delta$  increases as the magnetic field is tilted to higher angle. Note that Ref. 24 also quotes high  $|g^*|$  values in the range 5–9. From a wider perspective, similar conclusions regarding the necessity of a proper inclusion of the exchange interaction have been reached before in other recent works on square QWs<sup>11,14</sup> and PQWs.<sup>7</sup> Interestingly, a recent theoretical investigation based on density functional theory<sup>8</sup> going beyond a Hartree calculation and treating  $g^*$  as an input parameter, which attempts to reproduce the ring structures seen in Refs. 7 and 14, is only in qualitative agreement with the experiments.

Reference 8 also raises another open question. In the original investigations of Piazza *et al.*<sup>9</sup> and De Poortere *et al.*<sup>10</sup> on quantum Hall ferromagnets, hysteresis effects were observed in the longitudinal magnetoresistance at low temperature (seen most clearly below  $\sim 0.3$  K). However, in subsequent works, which are more similar to our situation, no hysteresis effects were reported.<sup>7,11,14</sup> Consequently, for

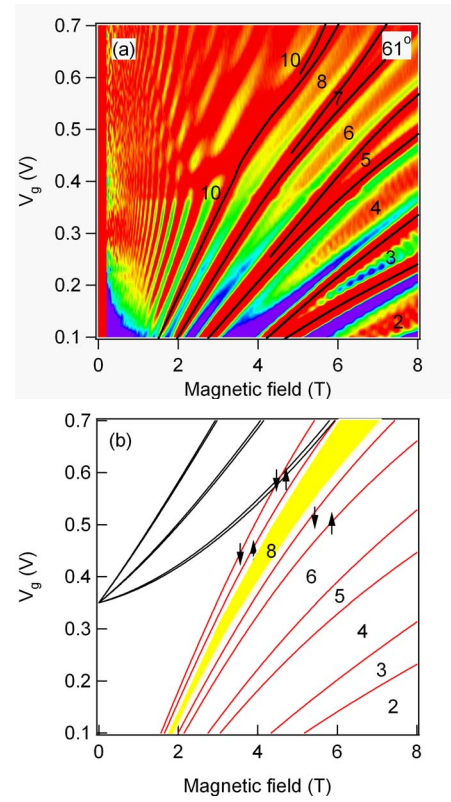


FIG. 7. (Color online) (a) Fan chart of  $\delta^2 V_{xx}$  in a tilted magnetic field of  $61^\circ$  constructed similar to the one in Fig. 3(a). (b) The calculated fan chart for this angle with first subband effective  $g$  factor  $|g^*|=9$  and taking  $|g_0|=0.44$ . The calculated fan chart reveals an anticrossing for  $\nu=8$  that occurs near the top right corner of the figure.

our relatively high (1.3 K) measurement temperature, we did not seek evidence for hysteresis effects.

#### IV. CONCLUSIONS

Our clear observation by transport measurements of the anticrossing between the first and second subbands for  $\nu=4$  at a finite tilt angle of  $21^\circ$  and the characteristic negative (positive) curvature of the first (second) subband LLs at this tilt angle and steeper tilt angles is seen to be qualitatively consistent with the theoretical predictions of Merlin,<sup>17</sup> but more theoretical work is needed to elucidate the underlying physics of the spin dependent transport in PQWs, and proper inclusion of the exchange and correlation effects is necessary.

Thus, PQWs not only form an ideal system for spintronics applications and theoretical investigations, but also display a rich hierarchy of physical phenomena in normal and tilted applied magnetic fields. Our second-differential Shubnikov–de Haas measurements have revealed that, depending on the tilt angle and magnitude of the applied fields, quantum Hall ferromagnetic ground states can be formed and

a series of intersubband crossings and anticrossings can occur. Furthermore, in such wide wells, these complex phenomena do not apparently require the use of ultrahigh mobility samples nor millikelvin temperatures for their observation. The high resolution of the second-differential method, as has been demonstrated here, indicates its usefulness in quantum Hall effect transport measurements.

## ACKNOWLEDGMENTS

We would like to acknowledge fruitful discussions with S. A. Studenikin, and thank P. Chow-Chong and H. Tran for help with sample processing. G.Y. and D.G.A. are partly supported by the DARPA-QUIST program (DAAD 19-01-1-0659).

- 
- <sup>1</sup>G. Salis, Y. Kato, K. Ensslin, D. C. Driscoll, A. C. Gossard, and D. D. Awschalom, *Nature (London)* **414**, 619 (2001).
- <sup>2</sup>P. Pfeffer and W. Zawadzki, *Phys. Rev. B* **72**, 035325 (2005).
- <sup>3</sup>S. Lindemann, T. Ihn, T. Heinzel, K. Ensslin, K. Maranowski, and A. C. Gossard, *Physica E (Amsterdam)* **13**, 638 (2002).
- <sup>4</sup>M. Shayegan, T. Sajoto, J. Jo, M. Santos, and H. D. Drew, *Phys. Rev. B* **40**, 3476 (1989).
- <sup>5</sup>K. Ensslin, C. Pistitsch, A. Wixforth, M. Sundaram, P. F. Hopkins, and A. C. Gossard, *Phys. Rev. B* **45**, 11407 (1992).
- <sup>6</sup>G. M. Gusev, A. A. Quivy, T. E. Lamas, J. R. Leite, O. Estibals, and J. C. Portal, *Phys. Rev. B* **67**, 155313 (2003).
- <sup>7</sup>C. Ellenberger, B. Simovič, R. Leturcq, T. Ihn, S. E. Ulloa, K. Ensslin, D. C. Driscoll, and A. C. Gossard, *Phys. Rev. B* **74**, 195313 (2006). Some magnetoresistance results for tilted field up to  $\sim 35^\circ$  are shown, but no conventional LL fan diagrams are presented.
- <sup>8</sup>G. J. Ferreira, H. J. P. Freire, and J. C. Egues, *Phys. Status Solidi C* **3**, 4364 (2006).
- <sup>9</sup>V. Piazza, V. Pellegrini, F. Beltram, W. Wegscheider, T. Jungwirth, and A. H. MacDonald, *Nature (London)* **402**, 638 (1999).
- <sup>10</sup>E. P. De Poortere, E. Tutuc, S. J. Papadakis, and M. Shayegan, *Science* **290**, 1546 (2000).
- <sup>11</sup>K. Muraki, T. Saku, and Y. Hirayama, *Phys. Rev. Lett.* **87**, 196801 (2001).
- <sup>12</sup>T. Jungwirth and A. H. MacDonald, *Phys. Rev. Lett.* **87**, 216801 (2001).
- <sup>13</sup>J. Jaroszyński, T. Andrearczyk, G. Karczewski, J. Wróbel, T. Wojtowicz, E. Papis, E. Kamińska, A. Piotrowska, D. Popović, and T. Dietl, *Phys. Rev. Lett.* **89**, 266802 (2002).
- <sup>14</sup>X. C. Zhang, D. R. Faulhaber, and H. W. Jiang, *Phys. Rev. Lett.* **95**, 216801 (2005); X. C. Zhang, I. Martin, and H. W. Jiang, *Phys. Rev. B* **74**, 073301 (2006).
- <sup>15</sup>Some other relevant examples are Y. Guldner, J. P. Vieren, M. Voos, F. Delahaye, D. Dominguez, J. P. Hirtz, and M. Razeghi, *Phys. Rev. B* **33**, 3990 (1986); A. J. Daneshvar, C. J. B. Ford, M. Y. Simmons, A. V. Khaetskii, A. R. Hamilton, M. Pepper, and D. A. Ritchie, *Phys. Rev. Lett.* **79**, 4449 (1997); A. Sawada, Z. F. Ezawa, H. Ohno, Y. Horikoshi, Y. Ohno, S. Kishimoto, F. Matsukura, M. Yasumoto, and A. Urayama, *ibid.* **80**, 4534 (1998); K. J. Thomas, J. T. Nicholls, M. Y. Simmons, W. R. Tribe, A. G. Davies, and M. Pepper, *Phys. Rev. B* **59**, 12252 (1999); S. Tarucha, D. G. Austing, Y. Tokura, W. G. van der Wiel, and L. P. Kouwenhoven, *Phys. Rev. Lett.* **84**, 2485 (2000); S. F. Fischer, G. Apetrii, U. Kunze, D. Schuh, and G. Abstreiter, *Nat. Phys.* **2**, 91 (2006).
- <sup>16</sup>J. C. Mann, in *Two Dimensional Systems, Heterostructures, and Superlattices*, edited by G. Bauer, F. Kuchar, and H. Heinrich (Springer-Verlag, Berlin, 1984), p. 183.
- <sup>17</sup>R. Merlin, *Solid State Commun.* **64**, 99 (1987).
- <sup>18</sup>M. A. Brummell, M. A. Hopkins, R. J. Nicholas, J. C. Portal, K. Y. Cheng, and A. Y. Cho, *J. Phys. C* **19**, L107 (1986).
- <sup>19</sup>A. D. Wieck, J. C. Maan, U. Merkt, J. P. Kotthaus, K. Ploog, and G. Weimann, *Phys. Rev. B* **35**, 4145 (1987).
- <sup>20</sup>Y. J. Wang, Y. A. Leem, B. D. McCombe, X.-G. Wu, F. M. Peeters, E. D. Jones, J. R. Reno, X. Y. Lee, and H. W. Jiang, *Phys. Rev. B* **64**, 161303(R) (2001).
- <sup>21</sup>R. Borroff, R. Merlin, R. L. Greene, and J. Comas, *Superlattices Microstruct.* **3**, 493 (1987); R. Borroff, R. Merlin, J. Pamulapati, P. K. Bhattacharya, and C. Tejedor, *Phys. Rev. B* **43**, 2081 (1991).
- <sup>22</sup>G. Yu, S. A. Studenikin, A. J. SpringThorpe, G. C. Aers, and D. G. Austing, *J. Appl. Phys.* **97**, 103703 (2005).
- <sup>23</sup>H. L. Stormer, K. W. Baldwin, L. N. Pfeiffer, and K. W. West, *Solid State Commun.* **84**, 95 (1992). Note that we can measure  $\partial^2 V_{xy}$  but choose to discuss just  $\partial^2 V_{xx}$  since all the physics of interest is contained therein, and since  $dR_{xy}/dB$  is similar to  $R_{xx}$ , it follows that  $d^2 R_{xy}/dV_g^2$  is similar to  $dR_{xx}/dV_g$ .
- <sup>24</sup>D. R. Leadley, R. J. Nicholas, J. J. Harris, and C. T. Foxon, *Phys. Rev. B* **58**, 13036 (1998).